Direct measurement of lattice spacing on crystalline surface using scanning tunneling microscope and laser interferometry

Masato AKETAGAWA*, Pongpun RERKKUMSUP, Koji TAKADA
Tomonori WATANABE, Shin SADAKATA
Department of Mechanical Engineering, Nagaoka University of Technology
Kamitomioka 1603-1, Nagaoka, Niigata, 940-2188 JAPAN
Fax: +81-258-47-9770, *E-mail: masatoaa@vos.nagaokaut.ac.jp

I. INTRODUCTION

Since research activities in precision engineering and nanotechnology have progressed rapidly, a new length-measurement method with sub-nanometer resolution is required. Nowadays, laser interferometry is of industrial length standard. A lot of commercial interferometer are widely used in the industry. However, it is very difficult to determine arbitrary length with nanometer accuracy using the commercial interferometer, because it suffers from the nonlinearity problem of fringe interpolation[1,2]. On the other hand, a phase modulation homodyne interferometer, which can determine the optical path difference of wavelength times integer ($\lambda \times n$) with the accuracy of 10 pm or less, has been proposed[3].

The lattice spacing of approximately 0.2 nm for some regular crystalline lattices is uniform and stable over a long range when the crystals are stress free. These crystals can be used as reference scales with sub-nanometer resolution instead of laser interferometry. X-ray interferometry (XRI) utilizing silicon crystal has been developed to determine the lattice spacing of silicon[4]. And it can be used for length measurement with sub-nanometer resolution[5]. However, XRIs are not commonly used in the industry, because they are special and relatively large instruments, and it is difficult to adjust it for obtaining sufficiently contrast x-ray fringes. On the other hand, the scanning tunneling microscope (STM)[6] is becoming a popular tool in surface engineering fields and can be used to obtain images of atoms on regular crystalline surfaces in air. It is, therefore, expected that such crystalline surfaces can be used as the "crystalline lattice scale" with sub-nanometer resolution by combining them with the STM as a detector[7-9]. We have shown the feasibility of the "crystalline lattice scale" using the crystal and a dual-tunneling-unit STM[9]. In order to realize a length measurement method using a crystalline surface[10], the lattice spacing on a regular crystalline surface, e.g. highly oriented pyrolytic graphite (HOPG), has to be measured and verified first. In this paper, a design and performance results for measuring the lattice spacing on a HOPG crystalline surface are discussed.

II. INSTRUMENT DESIGN AND OPERATION PRINCIPLE

Figures 1 shows a photograph of the instrument developed for measurement of lattice spacings on crystalline surfaces. The operations include; 1) three-dimensional atomic STM imaging of the crystalline surface of interest using a STM head with a *YZ*-axes tip scanner and an *X*-axis sample stage, 2) measurement of sample stage displacement along the *X*-axis (= measurement axis) with a phase modulation homodyne interferometer. If the number N of lattice spacings along measurement axis on the atomic STM image of the crystal and the sample stage displacement L along the measurement axis are determined, the lattice spacing d can be written as L/N. A low linear thermal expansion cast iron, whose coefficient less than 0.8×10^{-6} /K at room temperature, is selected for the material of the STM head and the base plate for the sake of a reduction of the thermal deformation effect. A tube-type PZT actuator is used for the *YZ*-axes tip scanner of the STM head. The STM head itself is supported with three precision screws. A

coarse approach of the STM tip into a tunneling region is performed by the Z-axis motion of the back precision screw which is attached to the base plate and a precise stepping motor. To enhance lateral and vertical rigidities of the STM head to the base plate, two springs are utilized. Four parallel springs are fabricated at the center of the base plate using a wire-cut method. The center part of the base plate is used as the X-axis sample stage with fine straight motion and high stiffness by combining the parallel springs and a stacked-type piezo actuator. The first resonance frequency of the parallel spring stage is over 2 kHz. The maximum travel of the stage is approximately 10 μm (applied voltage is 1 kV) with a maximum pitching or yawing error of less than 1.0 μrad. To adjust the sample surface to be parallel to the X-axis, a tilting sample adjuster, on which the sample should be placed, is set on the X-axis sample stage just beneath the STM tip. Three-dimensional STM imaging can be performed by combining the motions of the X-axis sample stage and the YZ-axes tip scanner. In order to reduce thermal drift error, the X-axis is selected as the measurement and fast scanning axis[11]. The instrument is also set in the thermo-stabilized cell[9], whose temperature stability is better than 0.05 K, to reduce the thermal drift. In the cell, calibrated thermo-, pressure- and humidity-meters are installed to determine the refractive index of air during the lattice measurement.

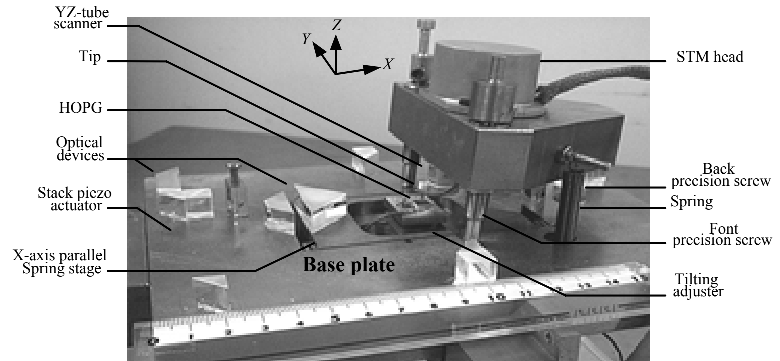

FIG. 1. The instrument for direct measurement of lattice spacing on crystalline surface. Dimensions (in mm) of the base plate and parallel spring stage are 200 (W) × 150 (D) ×25 (T) and 96 (W) ×52 (D) × 25 (T), respectively.

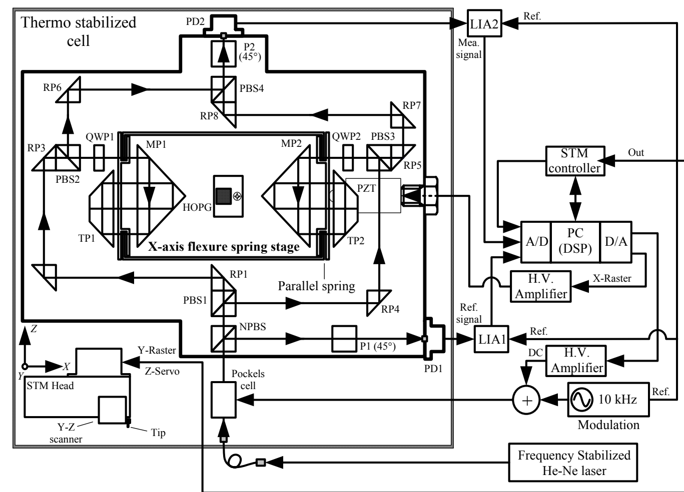

FIG. 2. Top schematic view of the instrument for direct measurement of lattice spacing on crystalline surface. NPBS: Non-polarizing beam splitter, PBS: Polarizing beam splitter, P: 45° polarizer, PD: Photodiode, RP: Right angle prism, QWP: Quarter wave plate, TP: Trapezoid prism, MP: Moving prism, LIA: Lock in amplifier.

Figure 2 shows the top schematic view of the measurement system. A linearly polarized beam, whose polarization angle is 45° from the vertical axis, is emitted form the frequency-stabilized He-Ne laser. The beam is introduced into the single mode polarization preserving fiber and led into the thermo-stabilized cell in order to reduce beam pointing instability and heating effect. The output beam from the end of the fiber passes through the Pockels cell. Two $LiNbO_3$ crystals of 5 mm × 5 mm × 20 mm size are utilized as the Pockels cell with a thermal-compensation configuration. The Pockels cell results in a phase modulation of a 10 kHz sinusoidal wave and bias-phase shift between the two polarization states p and s. The output beam from the Pockels cell passes through the non-polarizing beam splitter (NPBS), and a part

of the beam is split into the photodiode 1 (PD1) through polarizer 1 (P1; polarization angle = 45°) for the reference phase detection with the lock-in amplifier 1 (LIA1). The beam incident on the polarized beam splitter 1 (PBS1) is divided into two components, *p* and *s*. The output signal of LIA1 is used to control the bias-phase shift (= DC voltage) to the Pockels cell using 16 bit ADC and DAC with DSP so that the amplitudes of the *s* and *p* components at the PBS1 should be the same. The two beam components, *s* and *p,* travel along the two arms of the interferometer via PBS2/3, quarter wave plates 1 and 2 (QWP1/2), moving prisms 1 and 2 (MP1/2) on the *X*-axis stage and trapezoid prisms 1 and 2 (TP1/2). The beams travel back and forth four times between MP1/2 and TP1/2. The two beams which again pass through QWP1/2 and PBS2/3 are recombined at PBS4. The output beam from the PBS4 travels to PD2 via P2 (polarization angle = 45°). The PD2 signal is fed into LIA2 to determine the phase shift corresponding to the travel of the *X*-axis stage. The output signal of LIA2 should be a sine function of the optical path difference. The travel of the *X*-axis stage can be measured at the null points (= dark fringes) in the LIA2 signal with picometer resolution. In our design, the displacement for one fringe should be λ/16. The 16 bit ADC and DAC with DSP are also used for the recording of the LIA2 and tunneling current signals and the feed of the precise *X*-axis raster signal. The STM controller is used for the *Z*-axis servo control and the feed of the *Y*-axis raster signal.

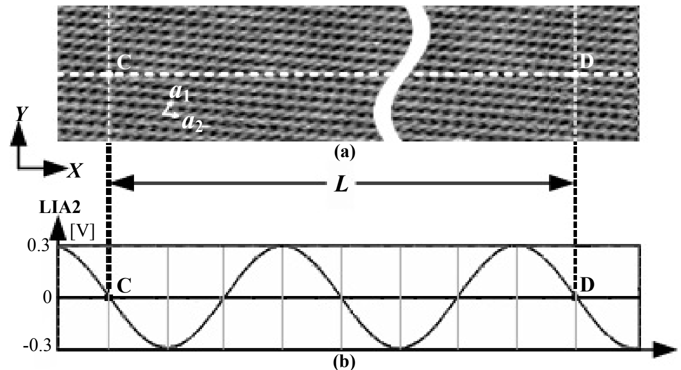

FIG.3. (a) A part of an approximately 100-nm-long atomic STM image of the HOPG crystal, (b) Output of LIA2 shown in Fig.2. One fringe equals λ/16. The complete 2 fringes of LIA2 output are compared with the number of crystalline lattices.

Table I. Experimental results for lattice spacing of HOPG.

No.	No. of atoms m_1 (atoms)	No. of atoms m_2 (atoms)	No. of atoms in scanning direction (atoms)	No. of fringes (cycles)	Calculated lattice spacing (nm)
1	204.5	164.3	320.0	2	0.247
2	205.8	165.7	322.4	2	0.245
3	205.3	165.2	321.5	2	0.246
4	204.3	164.9	320.3	2	0.247
Average					0.246 ± 0.002 (2σ)

III. PERFORMANCE EVALUATION AND RESULTS

The HOPG crystal is one of the candidate crystals for the "crystalline lattice scale". Therefore, the HOPG crystal was imaged and the lattice spacing on its surface was measured with the proposed instrument. Figures 3(a) and (b) show one of the results of the determination of the lattice spacing. Figure 3(a) shows the atomic STM image whose length along the *X*-axis (= measurement axis) was approximately 100 nm. Figure 3(b) shows the interferometer signal (LIA2) recorded for the center-line A-B parallel to the *X*-axis shown in Fig 3(a). In Fig. 3(b), the distance $\boldsymbol{L}$ between null points C and D corresponds to two fringes (≈ 80 nm). In Fig 3(a), two unit crystalline lattice vectors $\boldsymbol{a_1}$ and $\boldsymbol{a_2}$ are shown. In the case of the HOPG crystal, $|\boldsymbol{a_1}| = |\boldsymbol{a_2}| = d$ and the angle θ_{12} between $\boldsymbol{a_1}$ and $\boldsymbol{a_2}$ is 60°. Therefore, the number N of lattice spacings between null points C and D can be determined using vector calculation. The lattice spacing d, therefore, can be expressed as,

$$d = \frac{|\mathbf{CD}|}{N} = \frac{L}{\sqrt{m_1^{\,2} + m_2^{\,2} + 2m_1m_2\cos 60^\circ}}, \tag{1}$$

where m_1 and m_2 are constants in ***CD*** vector. The refractive index of air was determined from temperature, air pressure, humidity and the concentration of CO_2[12] using the modified Edlen method[13]. Table I summarized the measurements for the lattice spacing on the HOPG crystalline surface. Measurements were repeated four times within 2 hours. The mean value of the lattice spacing was very close to that in another reference[14]. The measurement uncertainty of *d* is come from the measurement uncertainties of *L* and *N*. From the uncertainty analysis, the expanded uncertainty (k = 2) for the measurement was 7 pm. Major contributors to measurement uncertainties from *L* include the Abbe offset error, deadpath error and reading error of LIA2 signal. Careful alignment when setting the sample and interferometer optics can reduce the Abbe offset and deadpath errors. The S/N ratio of the LIA2 signal was relatively low because we could not achieve better energy efficiency of the light in front of the fiber input due to a reflectance light effect. However, we will improve the S/N ratio 20-fold from the current one via accurate adjustment of the fiber and optical isolator. For *N*, although the thermal drift was relatively large in the measurement, the degree of uncertainty from it was not significant, because the fast scanning axis (*X*-axis) was selected as the measurement axis.

IV. CONCLUSION

In order to realize a length measurement method using a regular crystalline lattice as a reference scale, an instrument for direct measurement of the lattice spacing on regular crystalline surfaces using a STM and a phase modulation homodyne interferometer was developed. To demonstrate the performance of the proposed instrument, the lattice spacing on HOPG surface was measured, and the measurement uncertainty was evaluated. The experimental results show that the proposed method has high capability for lattice spacing measurement with high accuracy.

ACKNOWLEDGEMENTS

The partial financial support from the Scientific Research Fund of the Japanese Ministry of Education, Culture, Sports, Science and Technology is gratefully acknowledged. The partial financial support from Saneyoshi Scholarship Foundation and Mitutoyo Association for Science and Technology are also acknowledged.

REFERENCES

[1] C.M. Wu, and R.D. Deslattes, Appl. Opt. **37**, 28(1998), pp. 6696.
[2] F. Petru, and O. Cip, Prec. Eng., **23**, 1999, pp. 39.
[3] G. Basile, A. Bergamin, G. Cavagnero, and G. Mana, Metrologia, **28**, 1991/92, pp. 455.
[4] P. Becker, J. Stumpel, Metrologia, **27**, 1990, pp. 127
[5] G. Basile, P. Becker *et al.*, Proc. R. Soc. Lond. A, **456**, 2000, pp. 701
[6] G. Binnig, H. Rohrer, Ch. Gerber, and E. Weibel, Appl. Phys. Lett. **40**, 1982, pp. 178
[7] H. Kawakatsu, and T. Higuchi, J. Vac. Sci. Technol. A, **8**(1), Jan/Feb 1990, pp. 319.
[8] S. Gonda, H. Zhou, J. Fu, R.M. Silver, Proc. SPIE nanotechnology workshop, NIST, Oct, 2001.
[9] M. Aketagawa, K. Takada *et al.*, Meas. Sci. Technol. **9** (1998), pp. 1076.
[10] M. Aketagawa, P. Rerkkumsup *et al.*, Proc. of the 16th Annual Meeting, ASPE, Nov 2001, pp. 107.
[11] M. Aketagawa, K. Takada *et al.*, Rev. Sci. Instrument., **70**, 1(1999), pp. 133.
[12] J. Res. Natl. Inst. Stand. Technol. **104**, 225 (1999), pp. 225.
[13] K.P. Birch, and M.J. Downs, Metrologia, 1994, **31**, pp. 315.
[14] Sang-II Park, and C.F. Quate, Appl. Phys. Lett. **48** (2), 1986, pp. 112.